RAPID DEPLOYABLE ANTENNA CONCEPT SELECTION FOR CUBESATS

Maria Sakovsky[1], **Sergio Pellegrino**[1], **and Joseph Costantine**[2]

[1]*California Institute of Technology, Pasadena, CA, 91101 USA (msakovsk@caltech.edu; sergiop@caltech.edu).*
[2]*American University of Beirut, Beirut 1107 2020, Lebanon, and The University of New Mexico, Albuquerque, NM 87131 USA (jcostantine@ieee.org).*

ABSTRACT

In this paper, we present a new graphical tool for the preliminary design of deployable CubeSat antennas aimed at coupling electromagnetic and structural antenna design. The proposed methodology predicts antenna performance characteristics using analytical expressions and compares them graphically against antenna geometric parameters. Such a technique allows the comparison and analysis of several concepts simultaneously. A case study of preliminary antenna design in the Ka-band is included. The case study demonstrates the selection of constraint satisfying designs, the reduction of the design space by several orders of magnitude, and the identification of novel antenna concepts. A graphical user interface is created to implement the design methodology.

1. INTRODUCTION

Nanosatellite platforms have seen a recent popularity in providing low-cost access to space. Availability of off-the-shelf platforms such as CubeSats, kits available in multiples of 1U (a 10 cm cube), has broadened the capabilities of these satellites requiring high bit rate antennas for downlinking an increasing amount of data. Such antennas tend to be large in size, particularly at lower frequencies, and must be packaged for launch within the restricted CubeSat volumes. The majority of commercially available antennas for CubeSats are dipole/monopole and patch antennas, which while having significant flight heritage, cannot provide the gains and bandwidth required for new applications. Specific designs have been proposed in literature to address this gap. Several helical antennas have been developed such as those developed by Helical Communication Technologies and the Northrup Grumman Corporation with gains in excess of 3 dB and 10 dB, respectively [1, 2]. Designs for CubeSat parabolic reflectors have been developed such as the KaPDA antenna from the Jet Propulsion Laboratory [3], and the mesh reflector developed by BDS Phantom Works [4]. Concepts for other antenna types, including conical horns and the conical log spiral (CLS), have also been proposed [5, 6].

Deployable antenna design presents a coupled electromagnetic and structural problem. Electromagnetic performance is often predicted using numerical simulators such as Ansys Electronics Desktop [8], CST [9], or Feko [10]. To aid in the design process, catalogs of antenna types are available as add ons for these software tools. This includes the Antenna Magus tool [11], an add-on interface to CST and Feko, and the Ansys HFSS Antenna Design Kit [8]. However, electromagnetic performance is still evaluated manually for each antenna in the design space, which can be a lengthy process especially for large design spaces. On the other hand, structural performance is estimated using numerical simulators such as Abaqus [12]. Existing databases of material properties allow for rapid graphical comparison of material performance, as in the CES selector tool [13, 14]. The overall performance of the structure and packaging schemes, parameters critical to the problem, are not included in any database. Furthermore, several iterations between electromagnetic and structural simulations are required to converge on a final design, further lengthening the design process.

The above illustrates the need for a more integrated approach to deployable antenna design which evaluates electromagnetic and structural performance simultaneously. The novel methodology proposed here uses a graphical representation of antenna performance as a function of antenna geometry plotted on a set of two-dimensional axes. All antenna concepts of interest are compared on a common set of plots, allowing the designer to rapidly select those concepts that meet both electromagnetic and structural constraints. The result is a significantly reduced set of constraint satisfying designs without having relied on computationally expensive numeric simulations. The methodology is demonstrated for existing CubeSat antennas but is presented in a general way so it can be applied to new concepts as well.

The paper is arranged as follows. Section 2 presents the concept selection tool used to generate antenna comparison plots. Section 3 describes in detail the proposed design methodology to estimate performance and plot comparisons. Section 4 provides a case study of the use of this tool for the design of a high performance antenna for CubeSats operating in the Ka-band. Section 5 concludes the paper.

2. ANTENNA CONCEPT SELECTION TOOL

The proposed method approaches deployable antenna design through the following steps:

1. Select antenna operating frequency, f.
2. Identify a set of antenna types for comparison.
3. For each antenna type, select one or more packaging schemes. The combination of antenna type and packaging scheme is referred to here as an *antenna concept*.
4. Compute achievable antenna performance characteristics as a function of geometry for the selected operating frequency using analytic expressions.
5. Plot performance of every antenna concept as a function of geometry on a set of common two-dimensional plots.
6. Using the plot, select a narrow set of geometries that meet all requirements.

These steps have been implemented in Matlab to generate a user interface for collecting the input required by the steps above, as shown in Fig. 1. This tool can be used to compare the performance of any number of antenna concepts operating at a given frequency. This set of concepts can consists of different antenna types or can compare a single antenna packaged using several methods. The user can further specify which performance characteristics to use for comparison and optional values for requirements on these metrics. The output of the tool is a graphical comparison of antenna performance. The next section details the methodology for estimating and plotting antenna performance.

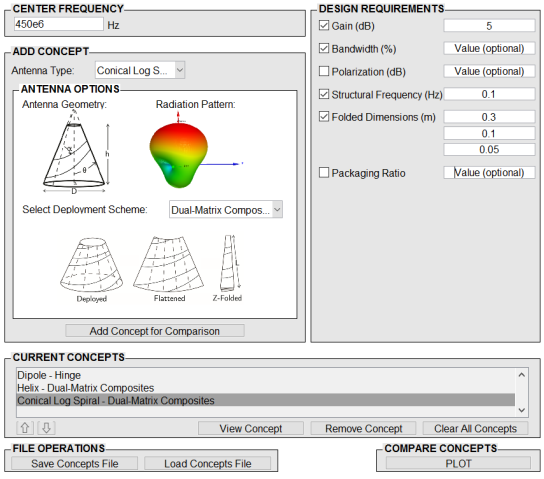

Figure 1. Interface implementing proposed method

3. METHODOLOGY

3.1. Antenna Types

Five antenna topologies have been selected to demonstrate the proposed methodology. These antenna types and their geometries are shown in Fig. 2. The commercial availability of dipole antennas in addition to its widespread implementation on CubeSats has made it a good reference design. Deployable helical antennas [1, 2, 15] and CLS antennas [7] constitute other major candidates proposed for CubeSat antennas. Concepts such as the parabolic dish and horn antennas are other possible candidates [3, 4].

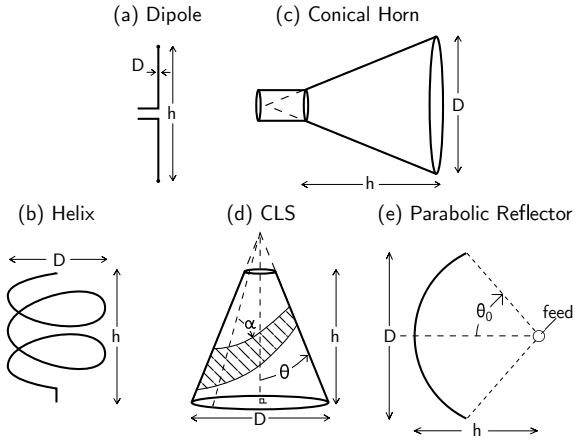

Figure 2. Geometry of antenna types selected for present study

As illustrated in Fig. 2, each antenna type is parametrized in terms of two geometric parameters: the antenna height, h, and its largest diameter, D. Limits on these parameters are derived from electromagnetic considerations which result in the desired radiation pattern for each antenna, for example a pattern that is directional [16]. The set of these limits define the initial design space for the problem. For the half-wavelength dipole, there is a unique h at which it operates. Constraints for the single helix are derived from desired operation in the end-fire mode. The horn geometry is defined to minimize antenna losses. The conical log spiral has experimentally obtained constraints on the cone angle, θ, and the conductor wrap angle, α, which ensure the radiation pattern is highly directional [17, 18]. These constraints can be translated to those on h and D by interpolation of this data. Finally, the constraints on the parabolic reflector dimensions result from optimization of aperture efficiency, ϵ_{ap}. Tab. 1 shows a summary of the constraints defining the initial design space.

3.2. Packaging Schemes

For this methodology, several structural elements common to many antenna packaging schemes are considered. The simplest of these is a *mechanical*

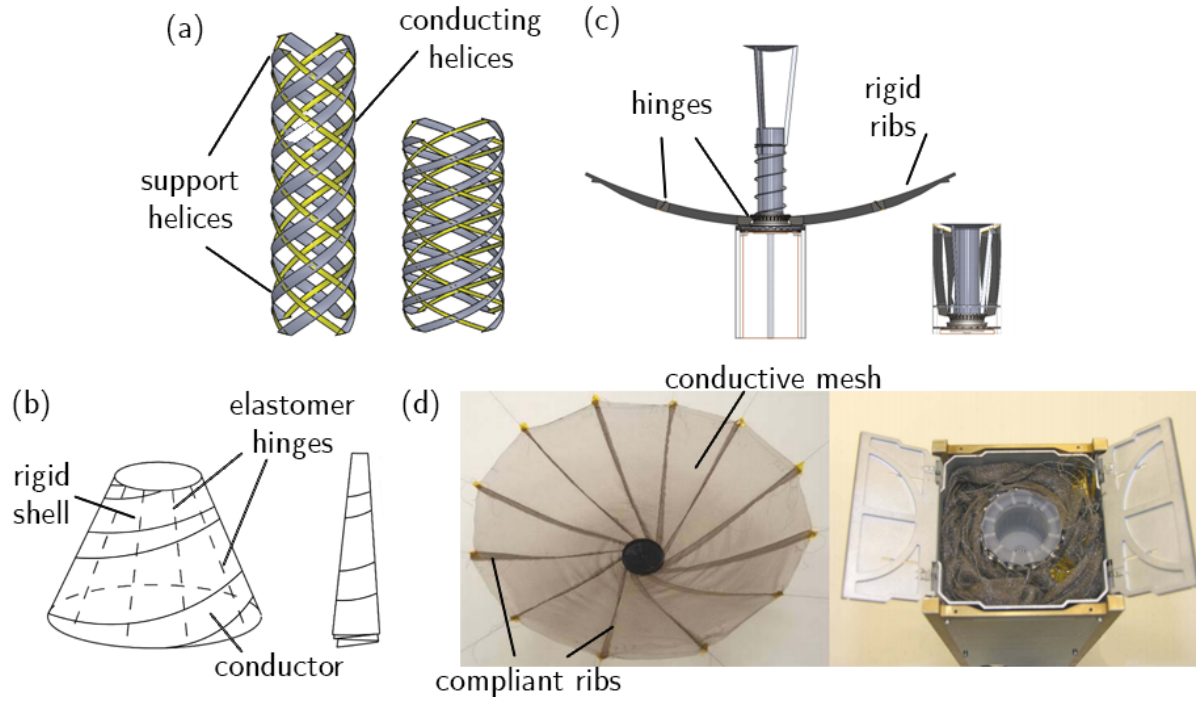

Figure 3. Packaging schemes used for CubeSat antennas (a) helical pantograph [15] (b) dual-matrix composite shell [5] (c) hinged ribs [3] (d) wrapped mesh [4]

Table 1. Initial design space for antennas in present study

Antenna Type	**Design Space**
Dipole	$h = \frac{\lambda}{2}$
Helix	$D = \frac{\lambda}{\pi}$ $\frac{3\lambda}{4}\tan 12^o < h < 20\lambda \tan 14^o$
Horn	$\tan 5^o < \frac{D}{2h} < \tan 30^o$ $h^2 = \left(\frac{D^2}{3\lambda}\right)^2 - \left(\frac{D}{2}\right)^2$
CLS	$2^o < 2\theta < 45^o$ $45^o < \alpha < 90^o$
Reflector	$0.65 < \epsilon_{ap} < 0.80$ $2\lambda < D < 50\lambda$

hinge supporting a stiff conducting element, suitable for the dipole antenna. For more complex architectures, packaging schemes often rely on two approaches: free-standing conductors supported by non-conducting elements, and conductors embedded in a non-conducting thin shell structure. Free-standing conductors, as those of the helical antenna, can be folded using *helical pantographs* where conducting helices are joined with opposite-sense non-conducting structural helices via scissor joints allowing the structure to compact elastically in the axial direction (Fig. 3a) [15]. The conductive elements can also be embedded in a *dual-matrix composite* shell, with soft elastomer matrix hinges arranged in an origami pattern (such as Z-folding) and a stiff epoxy resin elsewhere, providing structural rigidity (Fig. 3b) [6, 5]. This method is appropriate for cylindrical and conical structures.

Parabolic reflector antennas require unique packaging schemes due to the doubly curved surface of the main dish. Concepts proposed in literature use a conductive mesh reflector supported by curved ribs. The ribs can be stiff with several hinges allowing the reflector to fold alongside a central hub (Fig. 3c) [3]. Alternatively, the ribs can be made of compliant material and wrapped around a central hub using an origami packaging scheme (Fig. 3d) [4, 20]. Most of these packaged structures can deploy using stored strain energy reducing the cost and complexity introduced by actuated deployment schemes. A summary of antenna types and corresponding packaging schemes is given in Tab. 2.

Table 2. Antenna types and corresponding packaging architectures

Antenna Type	**Packaging Schemes**
Dipole	Mechanical Hinges
Helix	Helical Pantographs Dual-Matrix Composites
CLS	Dual-Matrix Composites
Horn	Dual-Matrix Composites
Reflector	Hinged Ribs Wrapped Mesh

Table 3. Design equations for electromagnetic performance metrics

Antenna Type	**Gain,** G	**Fractional Bandwidth,** BW (%)	**Polarization**
Dipole	1.643	3	linear
Helix	$\frac{15(\pi D)^2 h}{\lambda^3}$	56	circular
CLS	Interpolated from experiments in [18]	Interpolated from experiments in [18]	circular
Horn	$20\log\left(\frac{\pi D}{\lambda}\right) - \ell$ where $\ell = 2.912$ for optimum	$40 < BW < 75$	linear/circular
Reflector	$\left(\frac{\pi D}{\lambda}\right)^2 \epsilon_{ap}$	$5 < BW < 10$	Various

Table 4. Design equations for structural performance metrics

Antenna Type	**Packaging Scheme**	**Packaged Dimensions (m)**	**Packaging Ratio,** p	**Fundamental Frequency,** f_0
Dipole	Mechanical Hinge	$L_1 = h;\ L_2 = L_3 = D_{wire}$	1	$\frac{3.516}{2\pi h^2}\sqrt{\frac{EI}{\rho_l}}$
Helix	Helical pantographs	$L_1 = L_2 = 2\sqrt{\left(\frac{D}{2}\right)^2 + \left(\frac{h}{N}\right) - \left(\frac{D_{wire}}{2\pi}\right)}$ $L_3 = \frac{3}{2}hD_{wire}$	$\frac{D^2 h}{2ND_{wire}L_1}$	$\frac{D_{wire}}{4\pi D^2 N}\sqrt{\frac{E}{\rho(1+\nu)}}$
	Dual-matrix composites	$L_1 = h;\ L_2 = \frac{\pi D}{i};\ L_3 = 3ti$	$C_1 D$ $C_1 = 50\ \mathrm{m}^{-1}$	$\frac{3}{8\pi}\frac{h}{D}\sqrt{\frac{E}{\rho_a(1-\nu^2)}}$
Horn/CLS	Dual-Matrix Composites	$L_1 = g\left[1 + (\frac{D\cot\theta}{2h} - 1)\cdot (1 - \cos(\frac{\theta_0}{2i}))\right]$ $L_2 = 2g\frac{D\cot\theta}{2h}\sin(\frac{\theta_0}{2i});\ L_3 = 3ti$ $g = h\sqrt{\tan^2\theta + 1},\ \theta_0 = \frac{\pi h\tan\theta}{g}$	$C_2\frac{Dh}{\sqrt{h^2+\frac{D^2}{4}}}$ $C_2 = 133\ \mathrm{m}^{-1}$	$\frac{2h}{\sqrt{15}\pi D^2}(3 - 4\sin\left(\frac{3\theta}{4}\right))\cdot \sqrt{\frac{E}{\rho(1-\nu^2)}}$ where $\tan\theta = \frac{D}{2h}$
Reflector	Hinged Ribs	$L_1 = L_2 = \frac{D}{10}$ $L_3 = \frac{h}{2}\tan^{-1}\left\lvert\frac{\frac{h}{2D}}{(\frac{h}{D})^2 - \frac{1}{16}}\right\rvert$	$\frac{D^2 h}{L_1^2 L_3}$	$\min\left(\frac{2t^2}{\pi h^3}\sqrt{\frac{E}{\rho}}\frac{g_1}{g_2}, \frac{3}{8\pi}\frac{h}{D_{hub}}\sqrt{\frac{E}{\rho_{hub}(1+\nu)}}\right)$ $\frac{g_1}{g_2} = f(\theta_0)$ can be found in [19]
	Wrapped Mesh	$L_1 = \frac{\pi D}{i}$ $L_2 = L_3 = D_{hub} + 3t\cot(\frac{\pi}{i})$	$\frac{iDh}{4L_2^2}$	

3.3. Predicting Performance

The electromagnetic and structural performance characteristics of all antenna concepts presented in Fig. 2 and 3 can be predicted as a function of the geometry defined in Section 3.1. The electromagnetic performance is characterized by the maximum antenna gain, the fractional bandwidth, and polarization. These metrics indicate whether an antenna is capable of achieving the high bit rates required for an expanding number of CubeSat applications. These metrics are estimated using analytic expressions [16, 17] except for the CLS whose performance is predicted through interpolation of experimental data in [18]. Tab. 3 provides a summary of the equations used to predict electromagnetic properties. Note that the performance is predicted using only antenna geometry, and wavelength. Electromagnetic performance also depends on material parameters, feeding techniques, impedance matching and various other factors. However, making specific assumptions about these is acceptable in a preliminary design study.

The structural metrics used to gauge performance are the fundamental mechanical frequency of vibration in the deployed configuration, the packaged envelope dimensions, and the packaging ratio (defined as the volume enclosed by the deployed structure divided by the volume enclosed by the packaged structure). The fundamental frequency characterizes the stiffness of the structure in its softest mode of deformation and is a key metric of a structure's ability to achieve and maintain its deployed configuration. The other parameters characterize an antenna's ability to fit in constrained CubeSat volumes. A summary of the equations used to compute these metrics is given in Tab. 4. The fundamental frequency is estimated using expressions in [19] and the remaining metrics have been derived from [3, 5, 15, 20] or computed directly from antenna geometry. The structural met-

rics are predicted using antenna geometry, packaging geometry (conductor diameter, D_{wire}, number of folds in origami pattern, i, packaging hub diameter, D_{hub}, and number of conductor turns, N) as well as select material parameters (Young's modulus, E, Poisson's ratio, ν, the linear/areal density of conductors/thin shells, ρ, and material thickness, t). Specific assumptions have been made for material properties based on designs presented in literature.

3.4. Plotting Performance

The design problem is as follows: compare the performance of a set of n antenna concepts based on a set of m performance metrics. These parameters are selected by the user through the tool in Fig. 1. To facilitate direct comparison, the performance is plotted against antenna height, h, and diameter, D, on a set of two-dimensional plots. The algorithm used to compute performance is a brute force algorithm using four nested `for` loops over the antenna concepts, performance metrics, and all heights and diameters in the design space, , as illustrated in Fig. 4. The limits $h_{min}, h_{max}, D_{min}, D_{max}$ are computed from Tab. 1, and the metrics are evaluated using equations in Tab. 3 and 4.

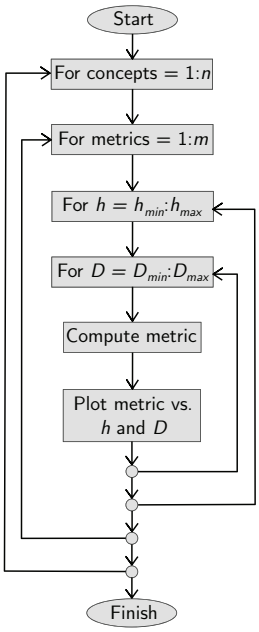

Figure 4. Algorithm used to estimate locus of antenna performance

This approach generates the chart illustrated by the schematic in Fig. 5, the layout of which was inspired by Ashby's quad charts used for material selection [13]. The top row of the chart plots m performance metrics against antenna height, while the bottom row plots m metrics against antenna diameter. Each ellipse represents a locus of achievable performance for a given antenna. Loci for all n antenna concepts are plotted on the same axes to allow comparison. Note that ellipses are only representative as the loci need not be convex or connected. Charts are arranged such that moving across plots, the y-axis remains constant, while moving down, the x-axis remains constant. This allows the user to track particular concepts across multiple plots, as illustrated by the red star in Fig. 5. Designs located inside the shaded region meet requirements for a particular metric.

By scanning all plots, one can identify designs that meet all imposed requirements and in this way obtain a narrow space of criteria-satisfying designs that is a subset of the original design space. A designer can start in the top left corner of the chart and select antenna heights that meet the requirement imposed on metric 1 for each antenna concept. Moving across the row allows the same to be done for each metric. Taking the intersection of the height ranges for each antenna concept, one can obtain a set of antenna heights that meet all requirements. A similar process applied to the bottom row results in a set of antenna diameters for each concept that meet all requirements.

This tool is not meant as a replacement to detailed numerical simulations but as a means of reducing time required for the preliminary design stage. It allows designers to easily compare performance of various antenna topologies against multiple packaging schemes in a single interface. It is assumed that the narrow set of constraint-satisfying designs is simulated in detail to finalize the concept.

4. CASE STUDY

A case study demonstrating the preliminary design of a deployable antenna operating at 30 GHz (Ka-band) is shown here. The Ka-band has the potential for higher bit rates and smaller antenna sizes [3]. However, it is also known to be susceptible to rain attenuation and requires higher surface accuracy than CubeSat antennas designed for the more commonly used UHF-band. The case study illustrates the use of the proposed concept selection methodology to explore a new design space and identify constraint satisfying concepts. The antenna concepts compared are:

1. Helix packaged using helical pantographs
2. CLS packaged using dual-matrix composites
3. Horn packaged using dual-matrix composites
4. Parabolic reflector packaged using hinged ribs

The following constraints are placed on the design:

1. Operation at 30 GHz
2. Maximum gain above 20 dB
3. Fundamental frequency higher than 0.1 Hz
4. Packaged antenna fits in a $10 \times 10 \times 5$ cm volume ($1/2$ 1U CubeSat)
5. Design maximizes bandwidth

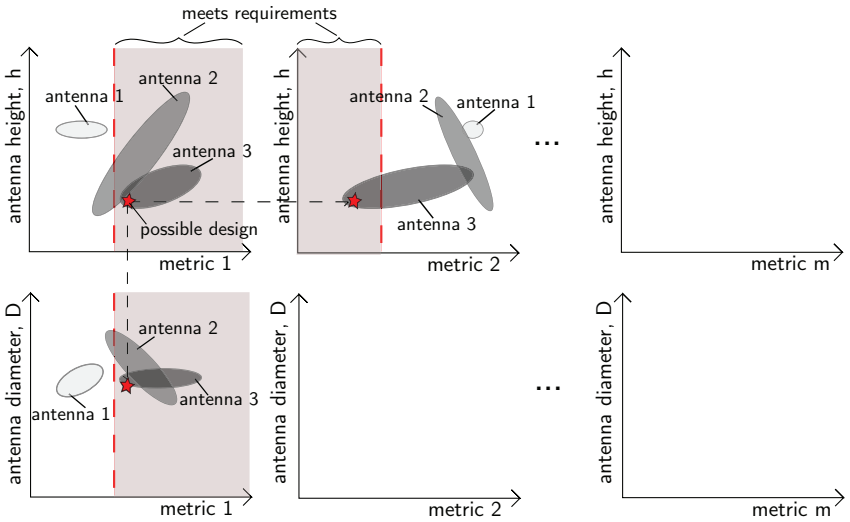

Figure 5. Schematic of chart used for antenna concept comparison

Following the methodology described in Section 3, design space limits are computed using Tab. 1 and the performance is estimated using Tab. 3 and 4. The results of the case study are generated using the tool in Section 2 and are plotted in Fig. 6. Starting from the top left corner of the chart (plot A1), one can select antenna heights for each concept which meet the gain requirement (i.e. ones in the shaded region with gain greater than 20 dB). It is evident that the entire loci of performance for both the helix and CLS antennas lie outside this region and hence cannot meet the gain requirements. However, from the performance loci for the horn and reflector one can see that there are designs that achieve the desired gain. In particular, horn antennas with $h > 6.0$ cm and reflectors with $h > 1.1$ cm meet the requirement.

Moving to the right, one can repeat the same process for plots A2-A6, obtaining designs that meet the bandwidth, frequency, and packaged volume requirements. As no quantitative requirement has been specified on the bandwidth, no new constraints can be derived from plot A2. However, it can be seen that the CLS maximizes the bandwidth. From plot A3, it is evident that all concepts lie in the shaded region and can meet the fundamental frequency requirements. Plots A4-A6 show that not all horn and reflector designs can be packaged in the required volume. From plot A4, one can get that $h < 9.5$ cm for the horn and $h < 16.0$ cm for the reflector. Plot A6 imposes a further constraint that $h < 14.5$ cm for the reflector. Designs that meet all requirements lie in the intersection of the inequalities derived from each plot. A similar process is repeated with the bottom row of the chart (plots B1-B6) to find antenna diameters that meet all requirements. This results is a narrow set of constraint-satisfying geometries as summarized in Tab. 5. The initial space has been reduced by at least an order of magnitude and the helix and CLS antennas have been ruled out as possible concepts as they cannot meet gain requirements.

Table 5. Initial design and optimization spaces for Ka band case study

Antenna Concept	**Initial Design Space (cm)**	**Optimization Space (cm)**
Helix	$0.2 < h < 4.0$ $D = 0.3$	Does not meet requirements
CLS	$0.3 < h < 35.2$ $0.2 < D < 3.4$	Does not meet requirements
Horn	$2.6 < h < 98.3$ $3.0 < D < 17.2$	$6.0 < h < 9.5$ $4.4 < D < 5.4$
Reflector	$0.6 < h < 31.0$ $2.0 < D < 99.9$	$1.1 < h < 14.5$ $4.0 < D < 50.0$

A horn antenna operating at the Ka-band has not previously been proposed in literature for deployment from CubeSats. However, Fig. 6 shows that it is a feasible concept for this design problem. The horn has less structural complexity than the reflector but can still achieve very high gains over a good bandwidth.

The next step in the design would involve detailed numerical simulations of the horn and reflector design in the optimization space in Tab. 5. This would be a much shorter process than if one started simulations from the initial design space without knowing if a particular concept could meet all requirements.

5. CONCLUSION

A novel methodology for rapid preliminary design of deployable antenna concepts for CubeSats is presented. Direct and quick comparison of the perfor-

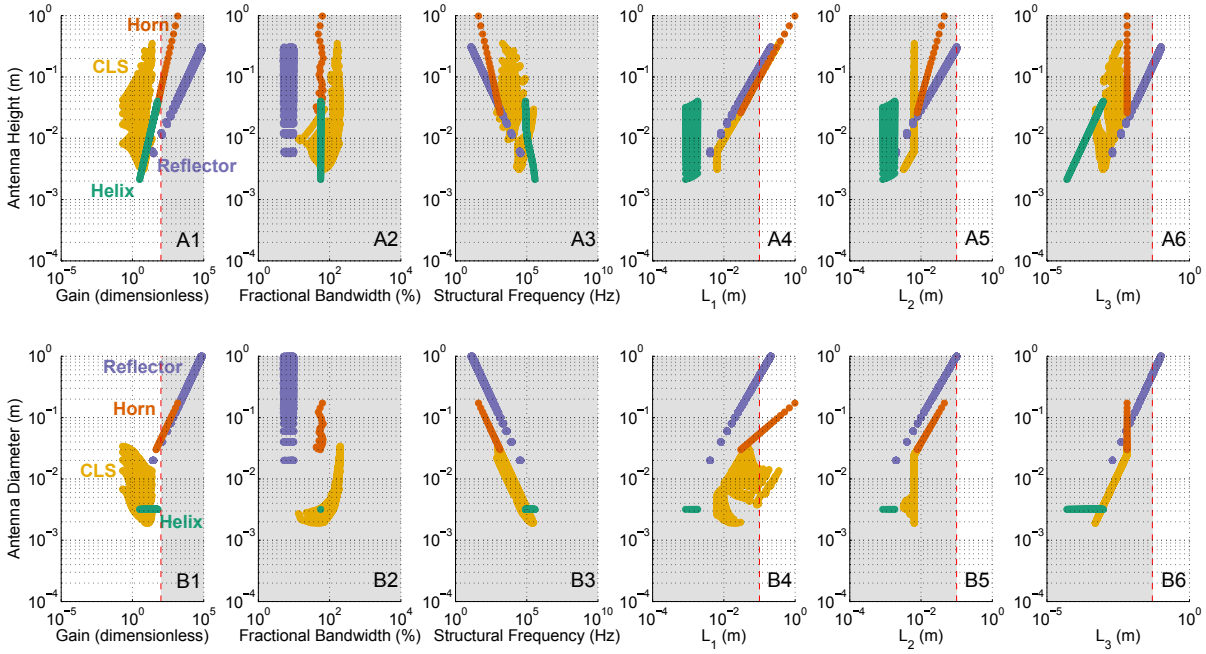

Figure 6. Case study at $f = 30$ GHz. From left to right, the plots shows antenna height/diameter as a function of gain, bandwidth, structural frequency, and the packaged antenna dimensions. The shaded regions represent areas of the plots that meet imposed requirements.

mance of many antenna concepts is enabled by plotting performance metrics against antenna geometric parameters. Achievable antenna performance is estimated using analytic expressions and experimental data instead of detailed numerical simulations. The methodology allows the antenna designer to identify antenna concepts meeting all design constraints and to select a narrow set of antenna geometries for more detailed performance simulations.

The methodology is demonstrated using a case study of an antenna design in the Ka-band. The technique allows the designer to quickly identify designs that cannot meet all requirements and achieve an order of magnitude reduction in the design space. It was further demonstrated that the tool proposed here can identify new antenna concepts.

The methodology has been demonstrated for a number of antenna types and deployment concepts which have been proposed in literature for use on CubeSats. The addition of other CubeSat antenna concepts proposed in literature will broaden the tool's impact. As the methodology is quite general, it can be applied easily to incorporate these new concepts. Integration of the methodology/concept selection tool with existing databases of antenna performance can significantly expand the utility of this method. Future work will also address the accuracy of this method by comparing case study results to antenna designs generated using standard numerical simulation methods.

ACKNOWLEDGMENT

This research was supported by the Air Force Office for Scientific Research (award no. FA9550-13-1-0061, program manager Dr. James Fillerup).

REFERENCES

[1] Helios Communication Technologies, *Helios Deployable Antenna*, available at: http://www.helicomtech.com/helios-deployable-series, 2016.

[2] D. Ochoa, K. Humer, and M. Ciffone, *Deployable Helical Antenna for Nano-Satellites*, 28th Annual AIAA/USU Conference on Small Satellites, Logan, Utah, 2014.

[3] J. Sauder, N. Chahat, M. Thomson, R. Hodges, and Y. Rahmat-Samii, *Ultra-Compact Ka-Band Parabolic Deployable Antenna for CubeSats*, Interplanetary CubeSat Workshop, Pasadena, California, 2014.

[4] C. S. MacGillivray, *Miniature Deployable High Gain Antenna for CubeSats*, 8th CubeSat Developers Workshop, San Luis Obispo, California, 2011.

[5] M. Sakovsky, I. Maqueda, C. Karl, S. Pellegrino, and J. Costantine, *Dual-Matrix Composite Wideband Antenna Structures for CubeSats*, AIAA Spacecraft Structures Conference, Kissimmee, FL, AIAA 2015-0944, 2015.

[6] G. M. Olson, S. Pellegrino, J. Constantine, and J. Banik, *Structural Architectures for a Deployable Wideband UHF Antenna*, 53rd

AIAA/ASME/ASCE/AHS/ASC Structures, Structural Dynamics and Materials Conference, Honolulu, Hawaii, 2012.

[7] J. Costantite, Y. Tawk, I. Maqueda, M. Sakovsky, G. Olson, S. Pellegrino, and C. G. Christodouou, *UHF Deployable Helical Antennas for CubeSats*, IEEE Transactions on Antennas and Propagation, vol. 64(9), p. 3752-3759, Sept. 2016.

[8] ANSYS HFSS Simulation Software, *ANSYS, Inc.*, available at: www.ansys.com/Products/Electronics/ANSYS-HFSS, 2016.

[9] Computer Simulation Technology Software, *CST*, available at: www.cst.com, 2016.

[10] FEKO Software, *Altair Engineering, Inc.*, available at: www.feko.info, 2016.

[11] Antenna Magus, *An Antenna Magus design case study*, available at: http://www.antennamagus.com/, 2016.

[12] Abaqus Software, Dassault Systmes Simulia Corp., Providence, RI, USA.

[13] M. F. Ashby, *Materials Selection in Mechanical Design*, 3rd ed., Oxford: Elsevier, 2005.

[14] Granta Material Intelligence, *Granta CES Selector*, available at: www.grantadesign.com/products/ces/, 2016.

[15] G. M. Olson, S. Pellegrino, J. Banik, and J. Costantine, *Deployable Helical Antennas for CubeSats*, 54th AIAA/ASME/ASCE/AHS/ASC Structures, Structural Dynamics and Materials Conference, Boston, MA, AIAA 2013-1670, 2013.

[16] C. A. Balanis, *Antenna Theory: Analysis and Design*, 4th ed., John Wiley & Sons, 2016.

[17] T. A. Milligan, *Modern Antenna Design*, 2nd ed., John Wiley & Sons, 2005.

[18] J. D. Dyson, *The Characteristics and Design of the Conical Log-Spiral Antenna*, IEEE Transactions on Antennas and Propagation, Vol 13(4), p. 488-499, 1965.

[19] R. D. Blevins, *Formulas for Natural Frequency and Mode Shapes*, 1st ed., Litton Educational Publishing, 1979.

[20] S. D. Guest, and S. Pellegrino, *Inextensional Wrapping of Flat Membranes*, Proceedings of the First International Seminar on Structural Morphology, p. 203-215, 1992.